Materials Research Express

PAPER

Modeling and optimization of operating parameters using RSM for mechanical behaviour of dual phase steels

RECEIVED
14 August 2019

REVISED
5 September 2019

ACCEPTED FOR PUBLICATION
10 September 2019

PUBLISHED
20 September 2019

E Olorundaisi , T Jamiru, T A Adegbola and O F Ogunbiyi
Department of Mechanical Engineering, Mechatronics and Industrial Design, Tshwane University of Technology, South Africa
E-mail: olorundaisiemmanuel@gmail.com

Keywords: surface hardness, ultimate tensile strength, optimization, modelling, dual phases steel

Abstract

In this study, the influence of operating parameters on the mechanical properties of Dual Phase (DP) steels was investigated, using response surface methodology (RSM) to develop a prediction model. In developing the model, temperature and holding time were considered as the model variables. To establish this fact, an experiment based on statistical four-level two factorial design method was carried out. Based on the statistical analysis, surface hardness (SH) shows a correlation coefficient of $R^2 = 0.9607$ while Ultimate Tensile strength (UTS) gave $R^2 = 0.9297$, this suggests that the proposed quadratic model is suitable for use. The optimum operating parameters were predicted using the user-defined design (UDD) under RSM and the result was confirmed through experiments, which predict at a temperature (T) of 800 °C and holding time (HT) of 60 min, hardness value was given as 157.798 HV and UTS as 553.648 Mpa. This result indicates that RSM is a suitable method to optimize the process variables for mechanical properties of DP steels.

1. Introduction

Over the years Dual-phase (DP) steels have drawn the attention of most researchers, basically in the automotive industries. This came as a result of the quest for safety, lightweight and energy-saving materials [1]. DP is made up of low carbon steels with a duplex ferrite-martensite microstructure [2–4]. When equated with other conventional steels, it is regarded as a dependable material for the automotive and other structural industries. DP steels are cost-effective and become the choice material due to its unique mechanical properties such as high tensile strength, excellent formability, improved continuous yielding behavior, crashworthiness, high hardenability and high strength-ductility [5–7].

Dual Phase steel has a polygon like microstructural shape and its properties is a function of T, holding time (HT), quenching rate, the chemical composition of the steel, fractional volume of ferrite to martensite, grain size and morphology of the steel [3, 8–10]. The distribution pattern of martensite also influences the mechanical behavior of DP steel. An isolated martensite region within the ferrite matrix tends to have improved strength and ductility than a distribution of chain-like structure surrounded by ferrite matrix [8].

Heat treatment plays a significant role in the formation of the microstructure of DP steels. Heating at Intercritical annealing to form ferrite-martensite structure when austenite fully transformed. However, the transformation of austenite is a function of temperature and HT [2, 5, 11]. At Intercritical annealing, the isothermal transformation of austenite to ferrite occurs, thereby forming an austenite-ferrite mixture. Hence, quenching of this mixture rapidly forms a ferrite-martensite microstructure [12]. The volume fraction of martensite is controllable by regulating the HT and temperature. Increase in temperature during Intercritical annealing results in the reduction of carbon in austenite leading to reduced martensite produced from austenite hence increase in HT may be responsible for improved properties as result of the segregation of substitutional atoms, therefore, increased temperature and HT varies directly with an increase in the volume fraction of austenite and directly proportional to the increasing volume of martensite when quenched rapidly [13]. However, at a high temperature, more volume fraction of austenite alongside a weaker carbon content is formed. Therefore, the carbon and other alloying elements present in DP steel affect its SH and hardenability [14–16]. Several types of

Table 1. Buildup information for RSM model.

File version	Design expert 11.1.2.0		
Study Type	Response Surface	Subtype	Randomized
Design Type	User-Defined	Runs	16
Design Model	Quadratic	Blocks	No Blocks

Table 2. Coded and actual operating conditions of the factors.

Independent variables	Units	Coded symbol	Type	Levels	L [1]	L [2]	L [3]	L [4]
Temperature	°C	A	Discrete	4	770	780	790	800
Holding Time	Min	B	Discrete	4	30	40	50	60

research have been carried out on DP steels, investigating its microstructure and mechanical properties, but little has been done on the optimization of its mechanical properties consideration [6, 16–19]. Therefore, in this study, UDD- RSM was applied to optimize the process parameters (Temperature and HT), in order to enhance the mechanical properties of DP steel. RSM is a statistical technique that involves the utilization of some experimental designs to develop mathematical models with linear, quadratic or interaction terms for optimum performance from given factors and response variables [20]. Adopting this technique reduces the number of experimental trials required to evaluate multiple parameters and their interaction. Table 1 shows the buildup information for the model.

2. Experimental detail

2.1. Design of experiment

Design of experiment (DOE) as stated earlier was carried out using UDD-RSM to optimize various parameters needed to improve the mechanical properties of DP steel. This technique combined the effect of mathematical and statistical techniques; however, this technique has been proven to be reliable by different researchers [21–25]. In this study, two parameters were controlled (temperature and HT), table 2 shows the coded and actual operating conditions of the factors. Two factors-four levels UDD was applied, and a total of 16 experimental runs were given, using Design Expert 11 software as shown in table 3 and a 95% confidence interval. The experimental results and statistical analysis data were analyzed using analysis of variance (ANOVA). Since the number of levels is just four, the appropriate model to adopt is the second-order polynomial model [26, 27] given in equation (1).

$$Y = \beta_0 + \sum_{j=1}^{k} \beta_j X_j + \sum_{j=1}^{k} \beta_{jj} X^2{}_j + \sum_{i}^{k} \sum_{<j=2}^{k} \beta_{ij} X_i X_j + e_i \quad (1)$$

Where:

Y is the predicted response
k the number of studied factors
Xi and Xj are the variables (factors);
β_0 is the constant-coefficient
β_j, β_{jj}, β_{ij} are the interaction coefficients of linear, quadratic and second-order terms
e_i is the error.

2.2. Material and heat treatment

Table 4 shows the chemical analysis of the as-received steel used in the present work. The samples are rectangular in shape and were wire cut to 17 samples each at a dimension of 10 × 2 mm. Using the DOE obtained, the experiments were performed, at a holding time of 30, 40, 50, and 60 min, the prepared samples were austenitized by heating to an Intercritical annealing temperature of 770 °C, 780 °C, 790 °C and 800 °C and quenched rapidly in bitumen for 10 min, followed by air cooling at room temperature for the complete removal of any traces of retained austenite and residual stresses.

Bitumen of grade SS 60–70 was heated to a temperature of 230 °C and used as quenching medium. The flashpoint of the bitumen was obtained to be 242 °C, using Pensky Martens close-cup flash point tester with facility for temperature reading. This value is below the flash point obtained from literature (250 °C or 276 °C) [28, 29],

Table 3. Design of experiments.

Run	Factor 1 A: Temperature (°C)	Factor 2 B: Holding time (Min)	Response 1 Surface hardness (HV)	Response 2 Ultimate tensile strength (Mpa)
1	800	50	151.23	535.976
2	790	50	150.89	532.76
3	790	40	146.08	520.87
4	770	30	141.26	508.97
5	780	40	145.98	518.29
6	800	60	158.32	561.1
7	770	60	152.33	528.09
8	770	50	147.78	521.76
9	780	30	143.56	510.36
10	780	50	148.25	529.56
11	800	40	144.33	511.522
12	790	30	143.96	511.08
13	790	60	156.92	560.67
14	780	60	154.89	553.89
15	800	30	147.07	521.233
16	770	40	143.89	513.56

Table 4. Chemical analysis of the low carbon steel.

Elements	C	Mn	Si	Al	Co	Cr	Cu	Ni	S	P
Composition (wt%)	0.094	0.54	0.093	0.036	0.002	0.039	0.14	0.048	0.02	0.016

this implies that the bitumen temperature must maintain a level below 242 °C during the experimental work, hence fire hazard will be inevitable. As a result, a temperature of 230 °C was maintained throughout the quenching cycle as a precaution towards fire disaster. By application of first law of thermodynamics, the mass of samples required to be quench without raising the bitumen temperature beyond 1 °C was determined. Two liters of stabilized bitumen was heated, in an aluminum pot, to a temperature of 230 °C. To estimate the mass of the steel samples that can be safely austempered in the bitumen at a given time, the following was considered:

Mass of sample, $= M_s g$

Mass of bitumen required, $M_b = 2000$ g

Mass of aluminum pot used, $M_a = 300$ g

Specific heat capacity of steel, $C_s = 0.42\ J\ g^{-1}K^{-1}$

Specific heat capacity of bitumen, $C_b = 3.9\ J\ g^{-1}K^{-1}$

Specific heat capacity of the aluminum pot, $C_a = 0.9\ J\ g^{-1}K^{-1}$

The temperature of the test sample from furnace, $T_1 = 800$ °C

$T_2 = 790$ °C

$T_3 = 780$ °C

$T_4 = 770$ °C

Initial Temperature of bitumen, $T_5 = 230$ °C

Final temperature of mixture, $T_6 = 231$ °C

Heat loss by steel $= M_s C_s (T_1\text{-}T_6)$

$= M_s{}^{*}0.42{}^{*}(800–231)$

$= 238.98\ M_s$ J

Heat gained by bitumen $= M_b C_b (T_6\text{-}T_5)$

$= 2000{}^{*}3.9{}^{*}(231–230)$

$= 7800$ J

Heat gained by aluminum pot $= M_a C_a (T_6\text{-}T_5)$

$= 300{}^{*}0.9(231–230)$

$= 270$ J

Total heat gained $= 7800 + 270$

$= 8070$ J

If no heat is lost to the surroundings, from the first law of thermodynamics [30],

Table 5. Mechanical properties of normalized low carbon steel.

Sample designation	Hardness (HV)	Ultimate tensile strength (Mpa)
Normalized sample	92.58	328.11

Heat lost by steel = Total heat gained

$238.98M_s = 8070$

$M_s = 33.7685$ g

The above analysis shows that 33.7685 g of steel at 800 °C is needed to cause the temperature of 2 liters of the bitumen to rise from 230 °C to 231 °C. this was repeated for temperature 790 °C, 780 °C and 770 °C and Ms of 34.3726 g, 34.9987 g, and 35.6480 g was obtained respectively. At no time during the experiment was the total mass of steel samples in the bitumen more than 17.8 g.

Before microstructural examination was done, the prepared samples were hot mounted with a Struers CitoPress-1 Machine. Proceeded by grinding and polishing of the samples face thoroughly, using Struers TegraPol-11 550 Machine, with disc grade of 90, 220 and 330 in successions. The samples were washed and air-dried, followed by etching with a 3% nital solution. The prepared samples surface was then placed under an Olympus microscope to capture the microstructure. The micro-hardness was determined using the Vickers indentation method at an applied load of 500gf with a time of 15 s. The surface hardness (SH) result was used in equation (2) to determine the ultimate tensile strength (UTS) of the samples. The Cahoon's expressions according to Vantyne (2015) [31] shows excellent agreement (<2%) in calculating the tensile strength. The expressions are given as:

$$\mathrm{UTS} = \left(\frac{H}{2.9}\right)\left(\frac{n}{0.217}\right)^{n} \tag{2}$$

Where:

UTS is given as Ultimate Tensile Strength

H is given as Surface Hardness

n is given as the Strain-Hardening Exponent (for low carbon steel it's given as 0.26) [32].

Converting hardness value from Vickers Pyramid Number (HV) to Megapascal (Mpa) is provided as:

$$\mathrm{Mpa} = (HV)(9.806) \tag{3}$$

3. Results and discussion

3.1. Mechanical analysis

The mechanical properties of the as-received sample are presented in table 5.

There is a uniform increase in strength as the HT increases. The increase could be due to the diffusion of more carbon content from supersaturated body cantered cell of ferrite in martensite to form secondary carbide phase [16]. The reduction in the Ultimate tensile strength (UTS) at a lower HT, could be as a result of higher percentage volume of austenite formation and reduction in the ferrite matrix or may be due to the effect of residual stress induced while quenching [16]. The value of UTS agrees with literature, which state UTS of DP steel ranges between 500 to 1200 Mpa [8]. Figure 1 shows the variation in the UTS and SH values of the experimental results. It was noticed that increment of SH and UTS is uniform and gradual not until the samples held at 50 and 60 min. Figure 2 represents the regression analysis of the samples for SH and UTS respectively, which indicates the significance and acceptability of the result as it is less than 1. It can, however, be stated that a prolong HT shows improved strength due to the formation of more austenite transforming into martensite [33–36].

3.2. Development of regression model equation for SH and UTS

Figures 3 and 4 show the individual behavior of the two factors used in improving mechanical properties of DP steel prediction. Figures 3(i)–(iv), shows the relationship between temperature, HT and SH. In figure 3(i), tremendous increase in SH value, at a constant temperature of 800 °C was discovered. As the temperature drops, the SH value also dropped, the rate of increasing SH in figure 3(iv), is steady tending towards a 180° line. This implies that with increasing temperature and holding time a better SH will be achieved. As stated above, the improved hardness could be related to a higher volume of austenite formation transforming into martensite and a consequent reduction in the ferrite matrix [16].

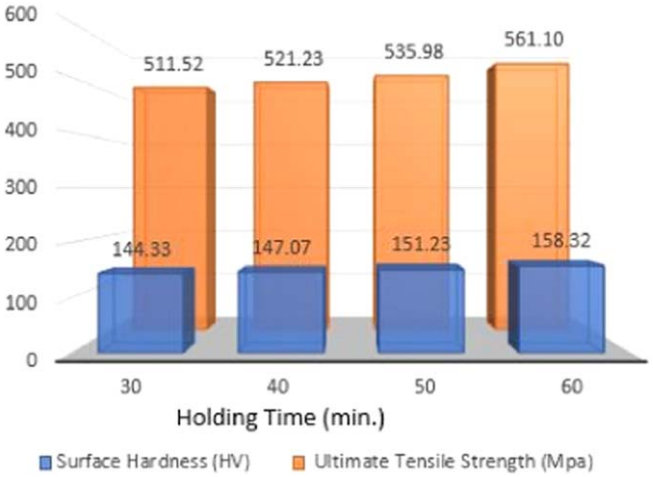

Figure 1. Variation in SH and UTS at different HT.

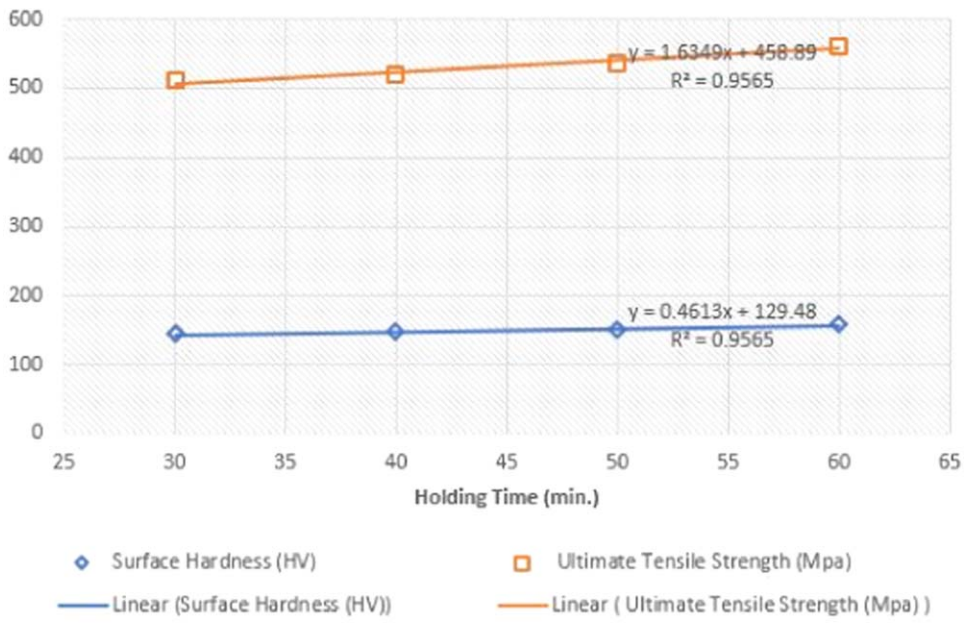

Figure 2. Regression analysis (R^2) for UTS and SH.

Likewise, in figures 4(i)–(iv), the hardness value increases at constant HT and increasing temperature. Figure 5(i) shows a sharp increase in UTS as compared to figure 5(iv). This result is in agreement with the experimental result in figures 1 and 2. As explained previously the change could be as a result of a higher percentage of austenite transforming into martensite and the interstitial diffusion of carbon that occurs rapidly.

Figures 6(i) and (ii) represents the perturbation plots, which shows the effect of all the factors at optimal experimental conditions. The plot helps to evaluate the effects of all the factors at a particular point in the design space. At a point where the curve obtained is sharp, the factor tends to be more important to the response. The plot was obtained for 785 °C temperature at a holding time of 45 min. Figure 6(i) shows that the response of SH efficiency was most sensitive to HT than temperature and likewise the response for UTS.

Figures 7(i) and (ii) represents the simultaneous increase in the values of holding time and temperature on SH and UTS. It depicts the influence of T and HT on the SH and UTS efficiency for DP steel. As seen, the interaction of the two variables was illustrated, as the T and HT increases, there is a corresponding increase in the SH and UTS. A maximum T and HT was reached at 800 °C and 60 min respectively, with a maximum SH and UTS of 158.32 HV and 561.1 Mpa respectively. Improved SH and UTS is noticeable with the T and HT separately represented but varies directly.

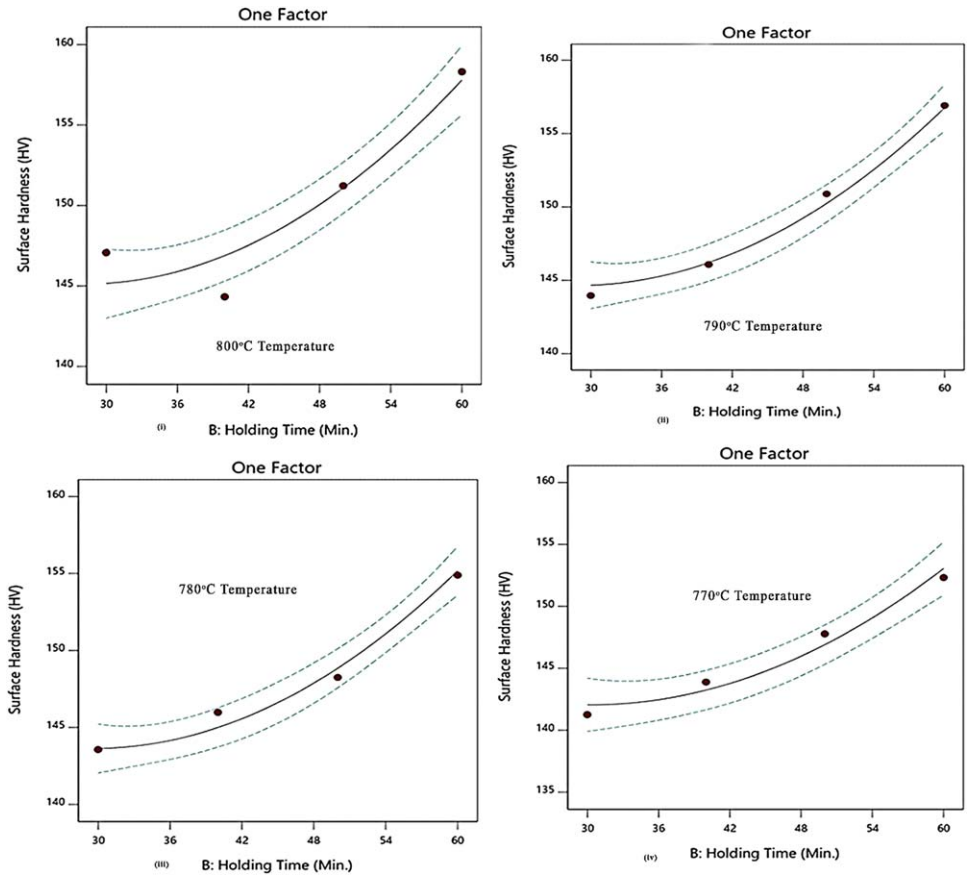

Figure 3. One factor interaction of the variables on SH at a constant HT.

The study of response surface and contour plots are represented in figures 8 and 9, it enables the optimization of parameters in enhancing the mechanical properties of DP steels. Figure 8(i) shows the response surface plot of SH efficiency, at a design point above the predicted value. The response surface of SH efficiency increased with a corresponding increase in HT and temperature. At an HT of 60 min and 800 °C temperature the maximum value of the SH efficiency was 158.32 HV, while in figure 8(ii), UTS efficiency was 561.104 Mpa.

3.3. Interaction of variables on SH and UTS

The design matrix of the 16 experimental runs alongside the coded factors for each variable was implored in determining all the constants in equation (1). A quadratic model for SH was used by the software for the response while cubic was selected for the UTS. The parameters were coded with four coding levels for each variable, as shown in table 2. Table 3 data were regressed by Design Expert 11.0 to develop a mathematical model for the coded and actual values. Second and third-order polynomial was used to correlate the response and variables values for HS and UTS respectively. The final equation in terms of coded and actual factors is represented in equations (4) and (5) respectively for SH, while equations (6) and (7) represent the final equation in terms of coded and actual factors for UTS respectively.

$$\text{Surface hardness} = 147.331 + 1.959*A + 5.91375*B + 0.4068*AB + -0.6075*A^2 + 2.79563*B^2 \quad (4)$$

$$\text{Surface hardness} = -1547.71 + 4.28824*\text{Temperature} + -2.14328*\text{Holding Time} + 0.001808*\text{Temperature}*\text{Holding Time} + -0.0027*\text{Temperature}^2 + 0.012425*\text{Holding Time}^2 \quad (5)$$

$$\text{UTS} = 524.681 + -0.0303384*A + 25.5243*B + 5.7223*AB + -4.95927*A^2 + 9.99824*B^2 + -7.83775*A^2B + 8.52321*AB^2 + 2.47698*A^3 + -2.15604*B^3 \quad (6)$$

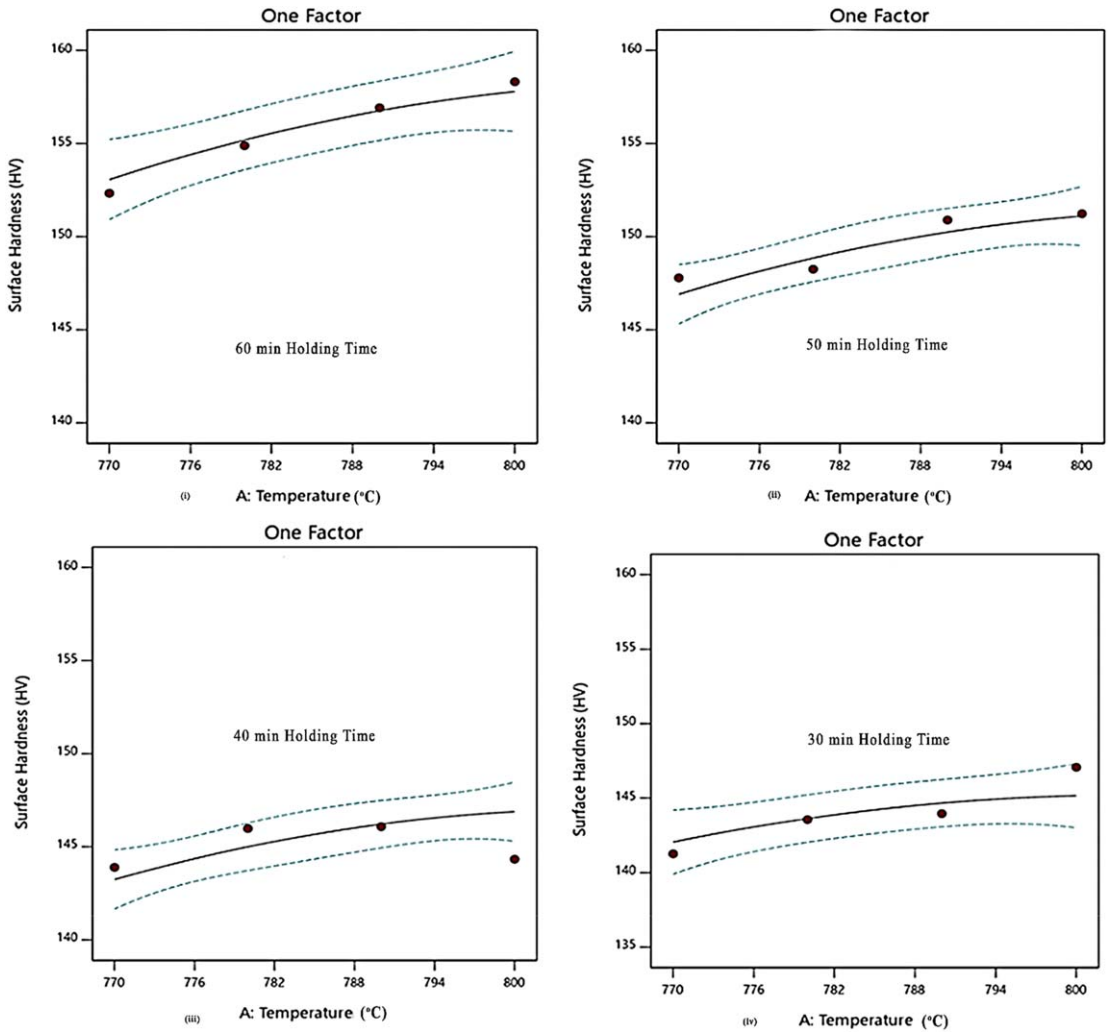

Figure 4. One factor interaction of the variables on SH at a constant temperature.

$$\begin{aligned} \text{UTS} = {} & -306727 + 1231.28*\text{Temperature} + -1278.78*\text{Holding Time} \\ & + 3.44415*\text{Temperature}*\text{Holding Time} + -1.64592*\text{Temperature}^2 \\ & + -1.85176*\text{Holding Time}^2 + -0.0023223*\text{Temperature}^2*\text{Holding Time} \\ & + 0.0025254*\text{Temperature}*\text{Holding Time}^2 + 0.00073392*\text{Temperature}^3 \\ & + -0.000638827*\text{Holding Time}^3 \end{aligned} \quad (7)$$

Where

A represent the coded value for temperature

B represent the coded value for holding time.

From equations (4) to (7), the positive sign represents synergy effect, while negative sign represents antagonistic effect. The coefficients with one factor of temperature and holding time represent the effect of that particular factor. The equations can be used to make predictions about the response for given levels of each factor. By default, the equation in terms of coded factors at the high levels of the factors are coded as +1 and the low levels are coded as −1, while for actual factor the levels are to be specified in the original units for each factor. The coded equation is useful for identifying the relative impact of the factors by comparing the factor coefficients. While the actual equation cannot be use because the coefficients are scaled to accommodate the units of each factor and the intercept is not at the center of the design space.

3.4. Model validation

The accuracy of the developed model can be validated from the value of R^2, Adjusted R^2 and standard deviation obtained. The value of R^2 described the significance and the acceptability of the developed model. If the

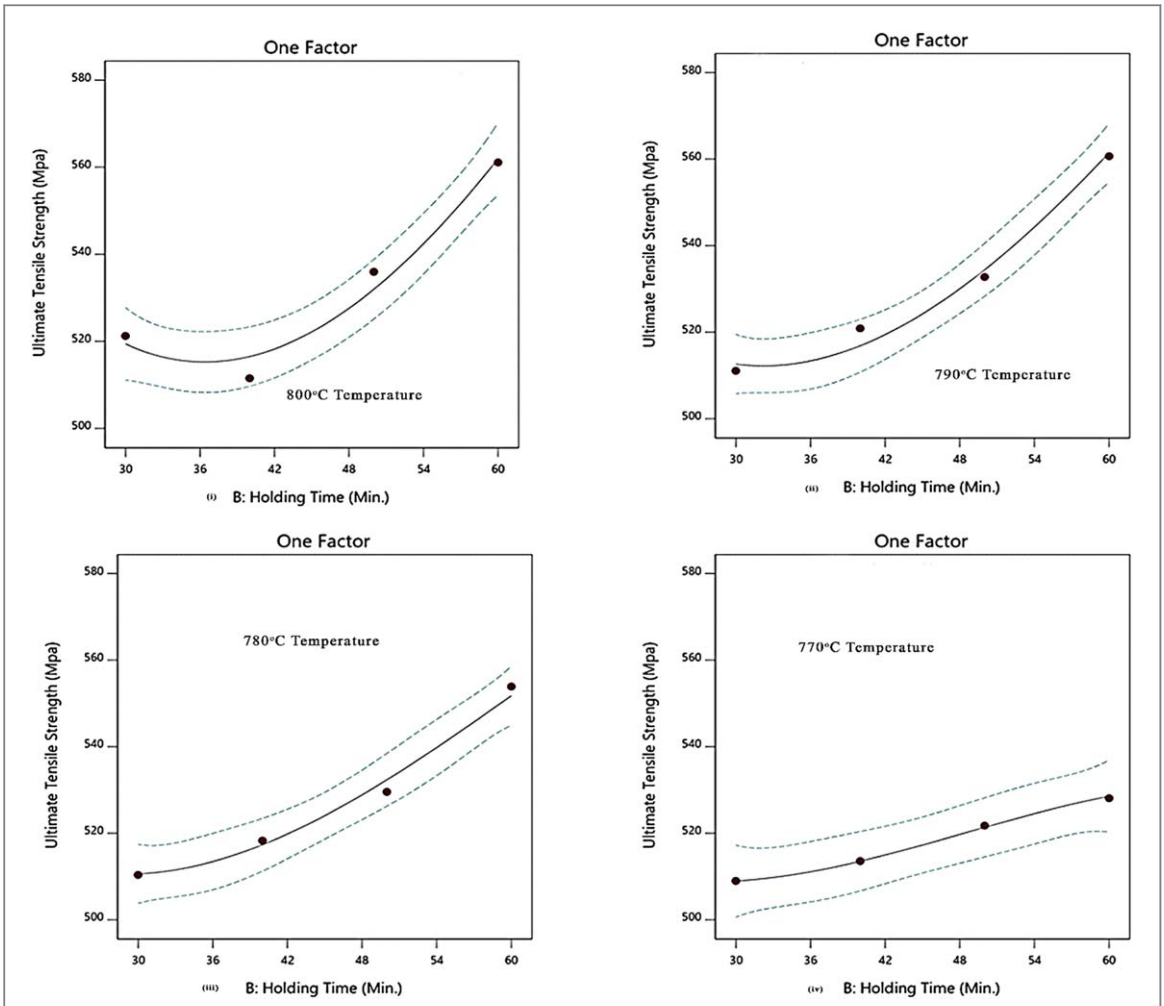

Figure 5. One factor interaction of the variables on UTS.

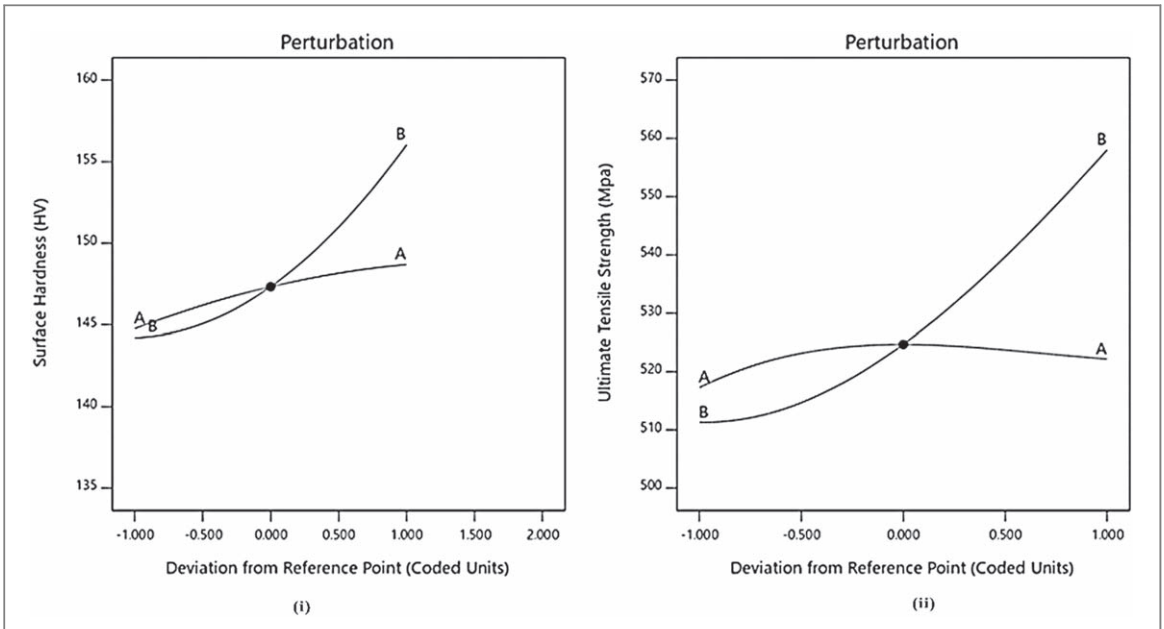

Figure 6. Perturbation plot for SH and UTS.

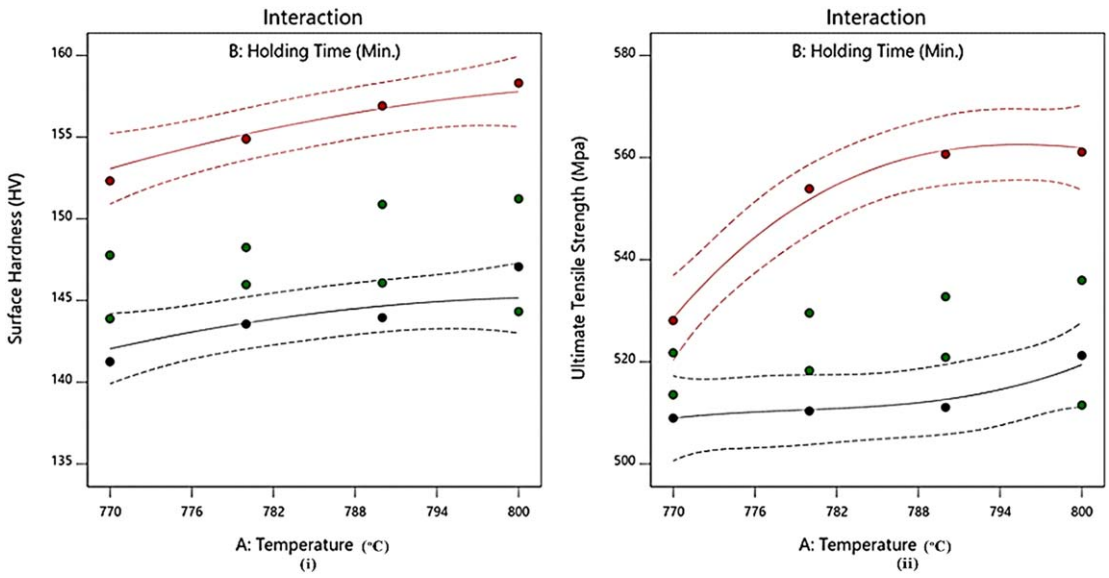

Figure 7. Interactions of variables on SH and UTS.

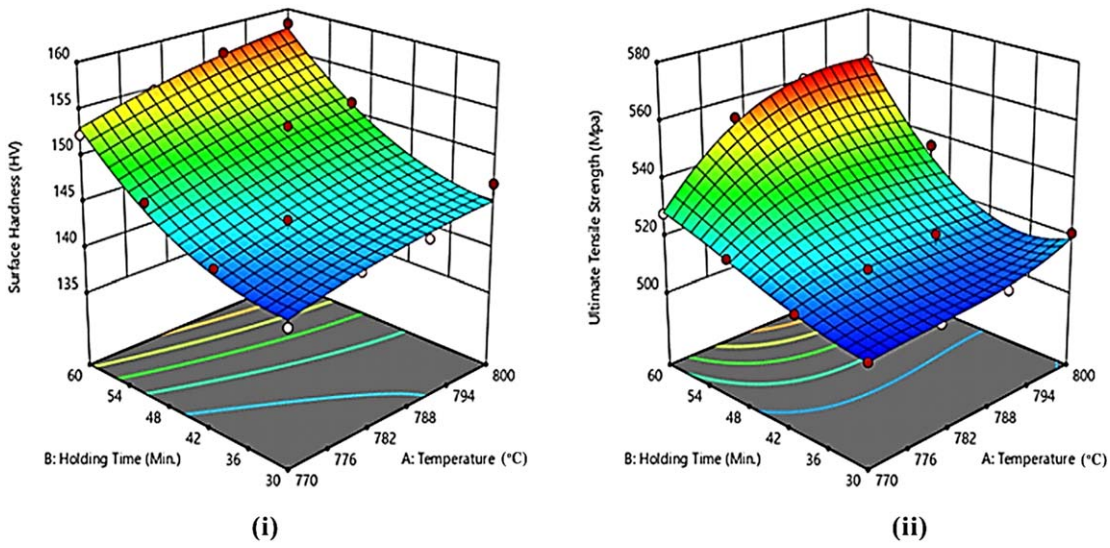

Figure 8. 3D Surface plot of interaction between holding time and temperature on SH and UTS.

difference between the Predicted R^2 and Adjusted R^2 is less than 0.2, the model can be said to be valid, likewise, the Adeq Precision which is the signal to noise ratio should be greater than 4 for an adequate signal. In this study; the difference between the Predicted R^2 of 0.8549 and Adjusted R^2 of 0.9411 is 0.0862, also the Adeq Precision ratio is 20.853 for SH. These values indicate that the model can be used to analyze the design space. For the UTS, the difference between the Predicted R^2 of 0.8678 and Adjusted R^2 of 0.9562 is 0.0884, also the Adeq Precision ratio is 18.325. This model can also be used.

Tables 6 and 7 shows the coefficients estimate in terms of the coded factors, it represents the expected change in response per unit change in factor value when all remaining factors are held constant. The intercept in an orthogonal design is the overall average response of all the runs. The coefficients are adjustments around that average based on the factor settings. When the factors are orthogonal the VIFs are 1; VIFs greater than 1 indicate multi-collinearity, the higher the VIF the more severe the correlation of factors. Figures 10 and 11 shows the relationship between the actual and the predicted response for SH and UTS.

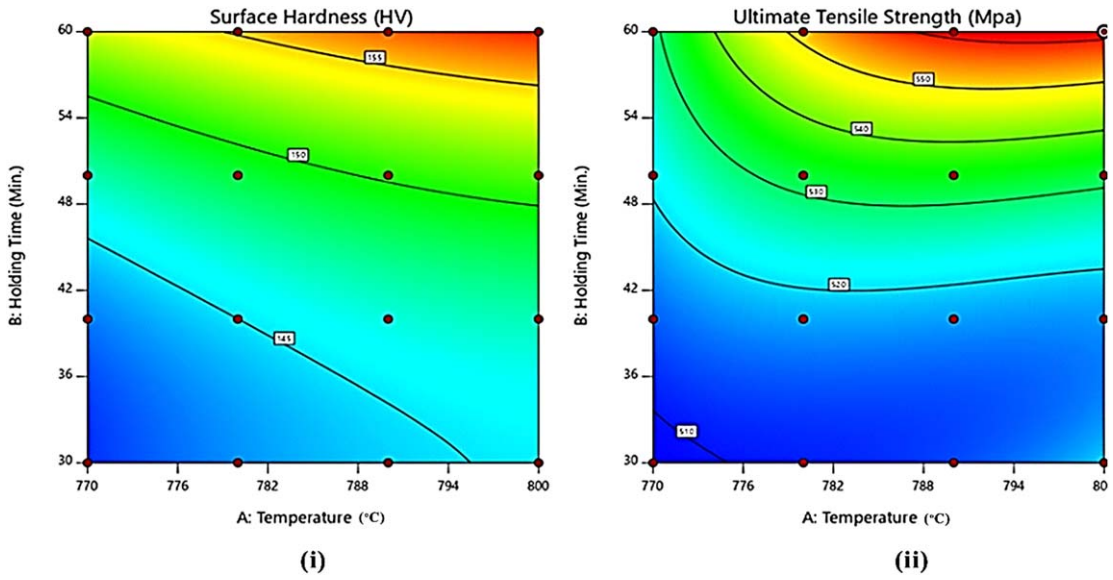

Figure 9. 2D Surface plot of interaction between holding time and temperature on SH and UTS.

Table 6. Coefficients in terms of coded factors for SH.

Factor	Coefficient estimate	df	Standard error	95% CI low	95% CI high	VIF
Intercept	147.33	1	0.6261	145.94	148.73	
A-Temperature	1.96	1	0.4136	1.04	2.88	1.0000
B-Holding Time	5.91	1	0.4136	4.99	6.84	1.0000
AB	0.4068	1	0.5549	−0.8295	1.64	1.0000
A^2	−0.6075	1	0.6936	−2.15	0.9379	1.0000
B^2	2.80	1	0.6936	1.25	4.34	1.0000

Table 7. Coefficients in terms of coded factors for UTS.

Factor	Coefficient estimate	df	Standard error	95% CI low	95% CI high	VIF
Intercept	524.68	1	1.86	520.14	529.23	
A-Temperature	−0.0303	1	4.63	−11.36	11.30	14.24
B-Holding Time	25.52	1	4.63	14.20	36.85	14.24
AB	5.72	1	1.65	1.69	9.75	1.0000
A^2	−4.96	1	2.06	−9.99	0.0761	1.0000
B^2	10.00	1	2.06	4.96	15.03	1.0000
A^2B	−7.84	1	2.76	−14.59	−1.08	2.56
AB^2	8.52	1	2.76	1.77	15.28	2.56
A^3	2.48	1	4.60	−8.78	13.74	12.67
B^3	−2.16	1	4.60	−13.42	9.10	12.67

3.5. ANOVA and statistical significance of the model

ANOVA was used to justify the integrity and significance of the model. P-values less than 0.1, implies that model term is significant. For SH, the Model F-value is 48.89 which implies that the model is significant. The P-values is <0.0001 therefore, A, B, B^2 are significant model terms. For UTS, the Model F-value is 37.42 which implies that the model is significant. The P-values is 0.0001 therefore, B, AB, B^2, A^2B, AB^2 are significant model terms. There is only a 0.01% chance that an F-value of 48.89 for SH and 37.42 for UTS could occur due to noise. Tables 8 and 9 shows the statistical analysis of the model, where the factor coding is coded, and the sum of squares is Type III-Partial.

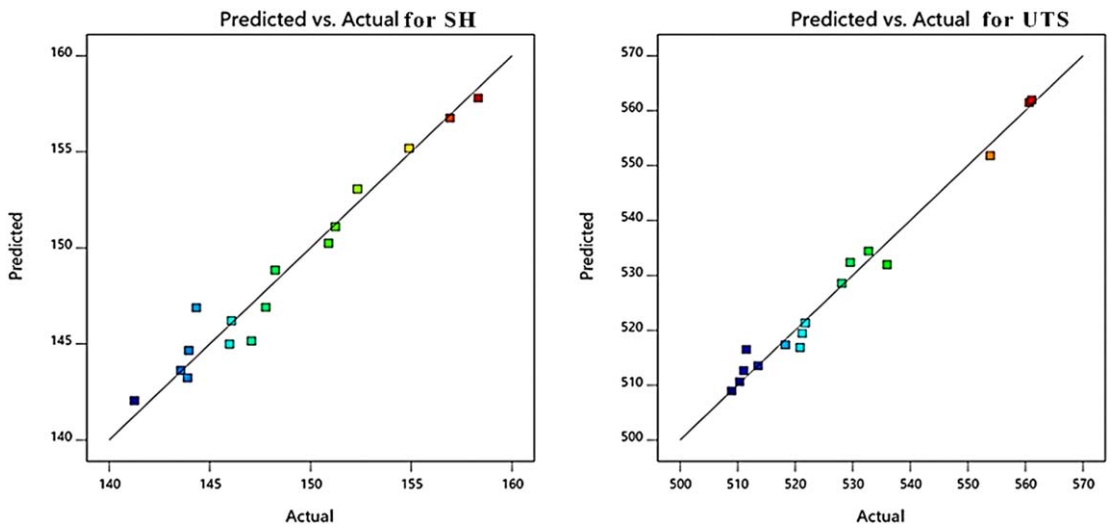

Figure 10. Predicted versus Actual Plots for SH and UTS.

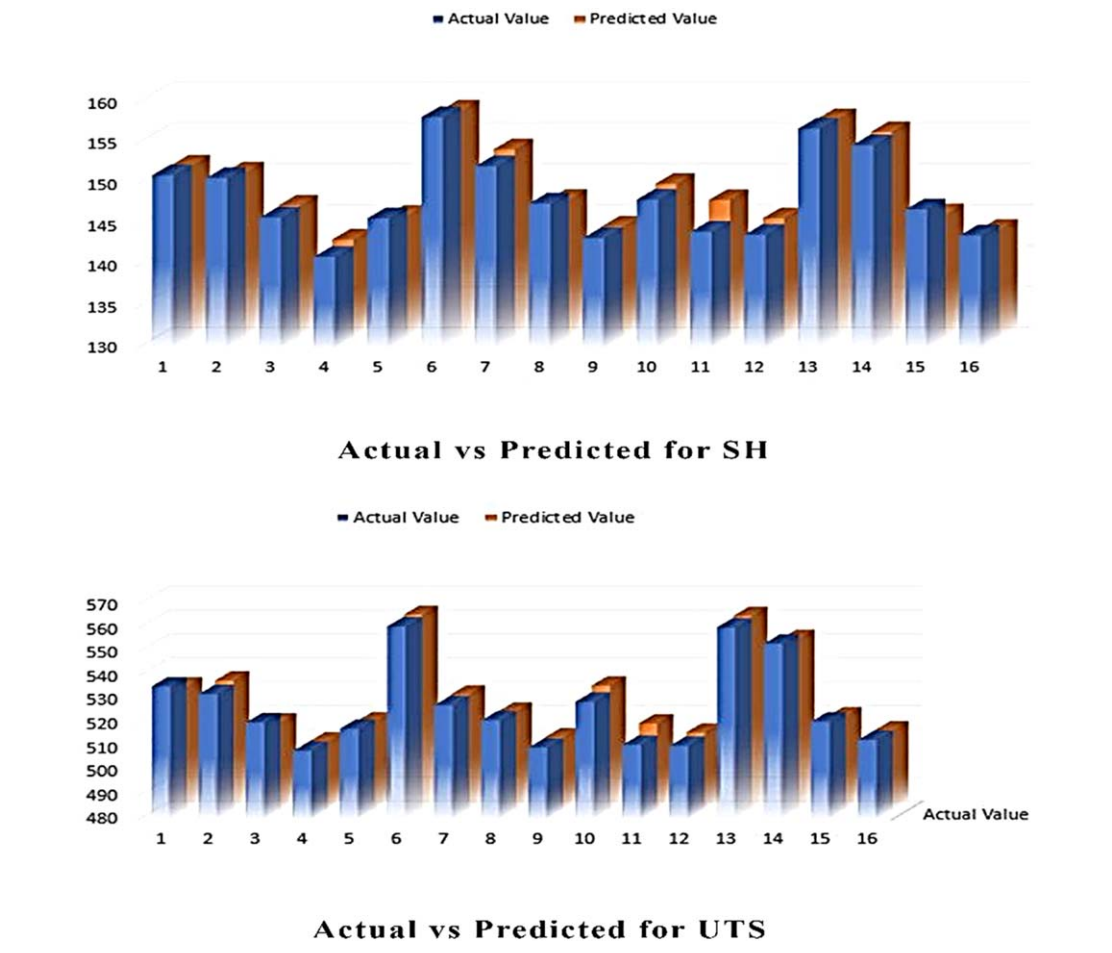

Figure 11. Comparison of Experimental and Predicted Results for SH and UTS.

3.6. Optimization studies

Optimization was carried out to maximized material strength, with the selected ranges of parameters (temperature and HT). At desirability of 0.399, seven solutions were obtained for optimum covering criterial. The first solution was selected as the best desirability for SH and UTS, as represented in figure 12. The report for the model is presented in tables 10 and 11 for SH and UTS respectively.

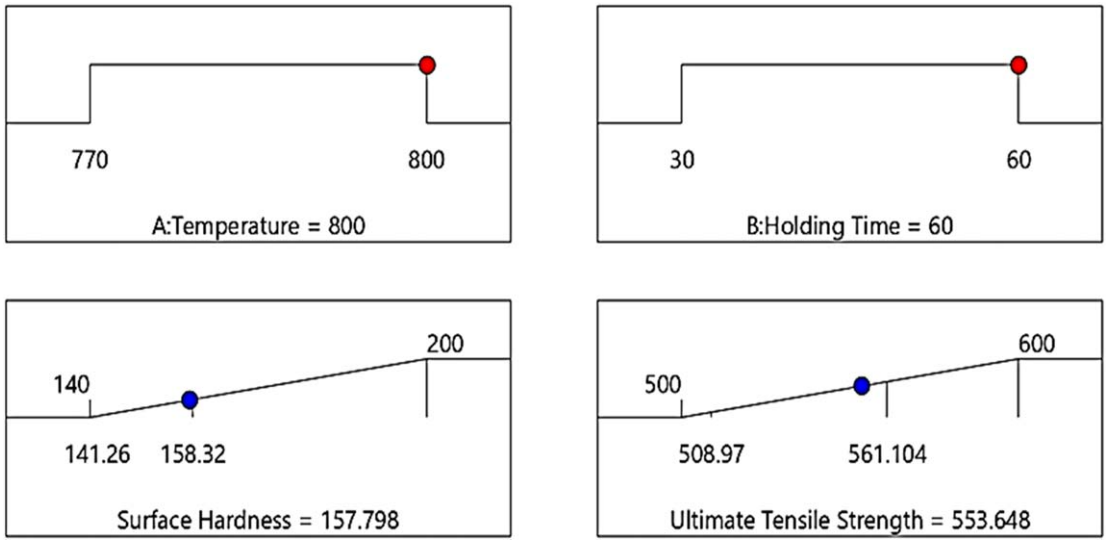

Figure 12. Optimization Result for SH and UTS.

Table 8. ANOVA for quadratic model for surface hardness.

Source	Sum of squares	df	Mean square	F-value	p-value	
Model	371.66	5	74.33	48.89	< 0.0001	significant
A-Temperature	34.11	1	34.11	22.44	0.0008	
B-Holding Time	310.87	1	310.87	204.47	< 0.0001	
AB	0.8172	1	0.8172	0.5375	0.4803	
A^2	1.17	1	1.17	0.7672	0.4016	
B^2	24.70	1	24.70	16.25	0.0024	
Residual	15.20	10	1.52			
Cor Total	386.87	15				

Table 9. ANOVA for cubic model for ultimate tensile strength.

Source	Sum of squares	df	Mean square	F-value	p-value	
Model	4507.09	9	500.79	37.42	0.0001	significant
A-Temperature	0.0006	1	0.0006	0.0000	0.9950	
B-Holding Time	406.78	1	406.78	30.39	0.0015	
AB	161.70	1	161.70	12.08	0.0132	
A^2	77.73	1	77.73	5.81	0.0526	
B^2	315.94	1	315.94	23.61	0.0028	
A^2B	107.86	1	107.86	8.06	0.0296	
AB^2	127.55	1	127.55	9.53	0.0215	
A^3	3.88	1	3.88	0.2898	0.6097	
B^3	2.94	1	2.94	0.2195	0.6559	
Residual	80.30	6	13.38			
Cor Total	4587.39	15				

4. Conclusion

Modeling and optimization of temperature and HT to improve the mechanical properties of DP steel was efficiently done, with a minimum experimental run of 16 using RSM. The behavior of each of the variables was observed on the SH and UTS, and it shows an inter−relationship between them; as the temperature and HT increase, there is a corresponding increase in the SH and UTS. From the results obtained from the Model; F- value, P-value, R^2, Predicted R^2, Adeq Precision and the comparison of the experimental and predicted values describe the accuracy of the model developed and can be used to navigate within the design space.

Table 10. Report of the SH model.

Run Order	Actual value	Predicted value	Residual	Leverage	Internally studentized residuals	Externally studentized residuals	Cook's distance	Influence on fitted value DFFITS	Standard order
1	151.23	151.10	0.1304	0.335	0.130	0.123	0.001	0.087	12
2	150.89	150.24	0.6468	0.215	0.592	0.572	0.016	0.299	11
3	146.08	146.21	−0.1303	0.215	−0.119	−0.113	0.001	−0.059	7
4	141.26	142.05	−0.7928	0.615	−1.036	−1.041	0.286	−1.315	1
5	145.98	144.99	0.9853	0.215	0.902	0.893	0.037	0.467	6
6	158.32	157.80	0.5217	0.615	0.682	0.662	0.124	0.837	16
7	152.33	153.07	−0.7367	0.615	−0.963	−0.959	0.247	−1.212	13
8	147.78	146.91	0.8696	0.335	0.865	0.853	0.063	0.605	9
9	143.56	143.63	−0.0676	0.335	−0.067	−0.064	0.000	−0.045	2
10	148.25	148.85	−0.5968	0.215	−0.546	−0.526	0.014	−0.275	10
11	144.33	146.89	−2.56	0.335	−2.542	−4.054[a]	0.542	−2.877[b]	8
12	143.96	144.66	−0.7024	0.335	−0.699	−0.679	0.041	−0.482	3
13	156.92	156.76	0.1589	0.335	0.158	0.150	0.002	0.107	15
14	154.89	155.18	−0.2939	0.335	−0.292	−0.278	0.007	−0.198	14
15	147.07	145.16	1.91	0.615	2.500	3.874	1.664[b]	4.896[b]	4
16	143.89	143.24	0.6509	0.335	0.647	0.627	0.035	0.445	5

[a] Observation with |External Stud. Residuals| > 4.00.
[b] Exceeds limits.

Table 11. Report of the UTS model.

Run Order	Actual value	Predicted value	Residual	Leverage	Internally studentized residuals	Externally studentized residuals	Cook's distance	Influence on fitted value DFFITS	Standard order
1	535.98	531.95	4.03	0.585	1.708	2.176	0.411	2.584[a]	12
2	532.76	534.41	−1.65	0.465	−0.618	−0.583	0.033	−0.543	11
3	520.87	516.86	4.01	0.465	1.497	1.726	0.195	1.609	7
4	508.97	508.94	0.0276	0.865	0.021	0.019	0.000	0.047	1
5	518.29	517.34	0.9481	0.465	0.354	0.327	0.011	0.305	6
6	561.10	561.94	−0.8392	0.865	−0.624	−0.589	0.250	−1.492	16
7	528.09	528.56	−0.4687	0.865	−0.349	−0.322	0.078	−0.814	13
8	521.76	521.35	0.4124	0.585	0.175	0.160	0.004	0.190	9
9	510.36	510.62	−0.2560	0.585	−0.109	−0.099	0.002	−0.118	2
10	529.56	532.35	−2.79	0.465	−1.041	−1.050	0.094	−0.979	10
11	511.52	516.50	−4.98	0.585	−2.114	−3.820	0.630	−4.535[a]	8
12	511.08	512.65	−1.57	0.585	−0.665	−0.630	0.062	−0.749	3
13	560.67	561.46	−0.7861	0.585	−0.334	−0.307	0.016	−0.365	15
14	553.89	551.80	2.09	0.585	0.889	0.870	0.111	1.033	14
15	521.23	519.44	1.80	0.865	1.335	1.454	1.143[a]	3.681[a]	4
16	513.56	513.53	0.0288	0.585	0.012	0.011	0.000	0.013	5

[a] Exceeds limits.

Acknowledgments

The fund provided by the National Research Foundation (NRF) program, South Africa, is greatly appreciated.

ORCID iDs

E Olorundaisi https://orcid.org/0000-0002-6842-6134
O F Ogunbiyi https://orcid.org/0000-0002-6260-450X

References

[1] Darabi A C, Chamani H R, Kadkhodapour J, Anaraki A P, Alaie A and Ayatollahi M R 2017 Micromechanical analysis of two heat-treated dual phase steels: DP800 and DP980 *Mech. Mater.* **110** 68–83
[2] Li Z, Wu D, Lü W, Yu H, Shao Z and Luo L 2015 Effect of holding time on the microstructure and mechanical properties of dual-phase steel during intercritical annealing *J. Wuhan Univ. Technol. Mater. Sci. Ed.* **30** 156–61
[3] Alibeyki M, Mirzadeh H and Najafi M 2018 Fine-grained dual phase steel via intercritical annealing of cold-rolled martensite *Vacuum.* **155** 147–52
[4] Xiong Z, Andrii K, Nicole S and Elena V P 2014 Effect of holding temperature and time on ferrite formation in dual phase steel produced by strip casting *Mater. Forum.* **38** 44–8
[5] Zuo X, Chen Y and Wang M 2012 Study on microstructures and work hardening behavior of ferrite-martensite dual-phase steels with high-content martensite *Mater. Res.* **15** 915–21
[6] Radwanski K, Kuziak R and Rozmus R 2019 Structure and mechanical properties of dual-phase steel following heat treatment simulations reproducing a continuous annealing line *Arch. Civ. Mech. Eng.* **19** 453–68
[7] Jamei F, Mirzadeh H and Zamani M 2019 Synergistic effects of holding time at intercritical annealing temperature and initial microstructure on the mechanical properties of dual phase steel *Mater. Sci. Eng.* A **750** 125–31
[8] Xiong Z P, Kostryzhev A G, Stanford N E and Pereloma E V 2015 Microstructures and mechanical properties of DP and TRIP steels after laboratory simulated strip casting *Mater. Des.* **88** 537–49
[9] Zamani M, Mirzadeh H and Maleki M 2018 Enhancement of mechanical properties of low carbon dual phase steel via natural aging *Mater. Sci. Eng.* A **734** 178–83
[10] Wu S, Wang D, Di X, Li C, Zhang Z, Zhou Z and Liu X 2019 Strength-toughness improvement of martensite-austenite dual phase deposited metals after austenite reversed treatment with short holding time *Mater. Sci. Eng.* A **755** 57–65
[11] Zeytin H K, Kubilay C and Aydin H 2008 Investigation of dual phase transformation of commercial low alloy steels: Effect of holding time at low inter-critical annealing temperatures *Mater. Lett.* **62** 2651–3
[12] Ashrafi H, Shamanian M, Emadi R and Saeidi N 2017 Examination of phase transformation kinetics during step quenching of dual phase steels *Mater. Chem. Phys.* **187** 203–17
[13] Xiong Z, Kostryzhev A G, Zhao Y and Pereloma E V 2019 Microstructure evolution during the production of dual phase and transformation induced plasticity steels using modified strip casting simulated in the laboratory *Metals (Basel)* **9** 449
[14] Hofinger M, Staudacher M, Ognianov M, Turk C, Leitner H and Schnitzer R 2019 Microstructural evolution of a dual hardening steel during heat treatment *Micron.* **120** 48–56
[15] Balbi M, Alvarez-Armas I and Armas A 2018 Effect of holding time at an intercritical temperature on the microstructure and tensile properties of a ferrite-martensite dual phase steel *Mater. Sci. Eng.* A **733** 1–8
[16] Gurumurthy B M, Sharma S S and Kini A 2018 Ferrite-bainite dual phase structure and mechanical characterization of AISI 4340 steel *Mater. Today Proc.* **5** 24907–14
[17] Nikkhah S, Mirzadeh H and Zamani M 2019 Fine tuning the mechanical properties of dual phase steel via thermomechanical processing of cold rolling and intercritical annealing *Mater. Chem. Phys.* **230** 1–8
[18] Jadudoma R and Khumkoaa S 2015 A study on phase transformation of hot rolled dual phase steel using deformation dilatometer *J. Eng. Appl. Sci.* **10** 190–6
[19] Scott C P, Shalchi Amirkhiz B, Pushkareva I, Fazeli F, Allain S Y P and Azizi H 2018 New insights into martensite strength and the damage behaviour of dual phase steels *Acta Mater.* **159** 112–22
[20] Atanas J P, Rodrigues C and Simmons R J 2015 Lean six sigma applications in oil and gas industry: case studies *International Journal of Scientific and Research Publications* **6** 540–4
[21] Saldaña-Robles A, Guerra-Sánchez R, Maldonado-Rubio M I and Peralta-Hernández J M 2014 Optimization of the operating parameters using RSM for the Fenton oxidation process and adsorption on vegetal carbon of MO solutions *J. Ind. Eng. Chem.* **20** 848–57
[22] Salam K K, Arinkoola A O, Oke E O and Adeleye J O 2014 Optimization of operating parameters using response surface methodology for paraffin-wax deposition in pipeline *Pet. Coal.* **56** 19–28
[23] Wang H, Cui X, Wang R and Li C 2012 Response surface optimization of the operating parameters for a complex distillation column based on process simulation *Energy Procedia* **16** 571–8
[24] Geyikçi F, Kiliç E, Çoruh S and Elevli S 2012 Modelling of lead adsorption from industrial sludge leachate on red mud by using RSM and ANN *Chem. Eng. J.* **183** 53–9
[25] Ramakrishnan R and Arumugam R 2012 Optimization of operating parameters and performance evaluation of forced draft cooling tower using response surface methodology (RSM) and artificial neural network (ANN) *J. Mech. Sci. Technol.* **26** 1643–50
[26] Raymond H M, Douglas C M and Christine M A-C 2009 *Response Surface Methodology* 3rd edn (New Jersey: Wiley)
[27] Yang K and El-Haik B 2003 *Design for Six Sigma: A Roadmap for Product Excellence* (http://alvarestech.com/temp/PDP2011/pdf/Design)
[28] Chin C 2005 Performance graded bitumen specifications *Sustain Infrastruct. Manag. Dep. ARRB.* **70** 1–10
[29] Bitumina. BITUMINA-BITUMEN-PENETRATION-GRADE-60-70-REV2 (www.bitumina.ae)
[30] Eastop T D and McConkey A 1993 *Applied Thermodynamics for Engineering Technologies* 5th edn (Harlow: Longman Group UK Limited) (http://www.pearsneduc.com)
[31] Pavlina E J and Van Tyne C J 2008 Correlation of yield strength and tensile strength with hardness for steels *J. Mater. Eng Perform* **17** 888–93
[32] Callister W D 2016 *Fundamentals of Materials Science and Engineering* 5th edn (New york city united States of America: Wiley)
[33] Amuda M O, Olaniyan T, Osoba L and Akinlabi E 2017 Mechanical properties of bitumen quenched dual phase steel *Sains Malaysiana* **46** 743–53
[34] Alabi A A, Obi A I, Yawas D S, Samotu I A and Stephen S I M 2012 Effect of water temperature on the mechanical properties of water quenched medium carbon steel *J. Energy Technol. Policy* **02** 04
[35] Adediran A A, Aribo S and Amuda M O H 2015 Mechanical properties of dual phase steel quenched in bitumen medium *Leonardo Electron. J. Pract. Technol.* **14** 1–16
[36] Alabi A A, Madakson P B, Yawas D S and Ause T 2013 Effect of bitumen on the mechanical properties of medium carbon steel *J. Miner. Mater. Charact. Eng.* **01** 131–7